BED SHEAR STRESS MEAUREMENTS OVER ROUGH FIXED AND MOBILE SEDIMENT BEDS IN SWASH FLOWS

Zhonglian Jiang[1] and Tom E. Baldock[1]

Direct measurements of bed shear stress have been conducted over rough fixed and mobile sediment beds in dam-break driven swash flows. The comparison between rough fixed and mobile bed results indicated the significant importance of grain borne shear stress component, induced by increased dispersive stress and the momentum transfer by moving sediment grains to the bed. The increase of the averaged peak bed shear stress under mobile sediment beds can be up to 100% of that for fixed beds. The direct incorporation of the shear stress data into the classic Meyer-Peter&Muller (1948) bed load model leads to over-estimate of bed load transport rate and reveals the fact of starved bed conditions applied in the present experiments.

Keywords: Bed shear stress; shear plate; fixed and mobile beds; dam break

INTRODUCTION

Bed shear stress plays an important role in the sediment transport modelling of the swash zone and thus the swash morphodynamics. Performance of the sediment transport models could be improved on basis of accurate bed shear stress data which has been rarely obtained so far. In the past several decades, various methods and instruments have been applied to investigate the characteristics of swash bed shear stress. The first and also the most straightforward way is the direct measurements of bed shear stress by using different kinds of sensors, e.g. shear plate (Riedel and Kamphuis, 1973; Rankin and Hires, 2000; Nemoto and Nishimura, 2000; Barnes et al., 2009; Seelam and Baldock, 2010; Pujara and Liu, 2014) or hot-wire/film probes (Li, 1994; Conley and Griffin, 2004; Sumer et al., 2011). The second conventional way is the velocity profile method which is based on the log-velocity profile assumption near the bed surface. A wide range of instrumentation have been developed to reach the objective of high-resolution velocity measurements within the boundary layer under different flow regimes, e.g. Laser Doppler Anemometry (LDA), Particle Image Velocimetry (PIV, e.g. Cowen et al., 2003), Acoustic Doppler Velocimetry (ADV, O'Donoghue et al., 2010) or Acoustic Doppler Velocity Profiler (ADVP, Puleo et al.,2012; Allis et al., 2014). However, challenges still exist. It is not easy to derive reliable velocity measurements due to the quickly developed swash boundary layer (Barnes and Baldock, 2010) and interactions between moving and non-moving grains, especially for natural conditions. Besides, the accuracy of the log velocity profile method highly depends on the deployment of the instruments. Considerable uncertainties will be caused by slight shifts in vertical height (Pope et al., 2006). Recent studies indicate that even the state-of-art instruments (e.g. ADV or ADVP) are not able to capture the shear stress variation at the initial stage which is of practical importance for the predictions of total sediment transportation. The third approach is the turbulent kinematic energy (TKE) method which requires accurate velocity measurements of one single fixed point within the boundary layer. But the influence of the acceleration and deceleration of the swash flow could not be overcome, neither for log-velocity profile method (Pope et al., 2006).

The shear plate method has been successfully applied to derive bed shear stress time series in the surf and swash flows (Barnes et al., 2009; O'Donoghue et al., 2010; Seelam and Baldock, 2010; Pujara and Liu, 2014). However its accuracy might be affected by misalignment in shear plate deployment, pressure gradient component and environmental vibration. Misalignment will lead to flow depression and separation, therefore generating extra forces on the shear plate (Hanratty and Campbell, 1996; Barnes et al., 2009; Kolitawong et al., 2010; Pujara and Liu, 2014). The pressure gradient contribution should be subtracted from the measured total bed shear stress. Barnes et al. (2009) investigated the pressure gradient component by using pressure transducers below the shear plate and ultrasonic displacement sensors above the shear plate, both of which indicate a similarly small magnitude. Moreover, some of the discrepancies observed in the direct bed shear stress measurements may be caused by the zero-position shift of the shear plate due to the disturbance of gate lifting. Considering the excellent performance of shear plates under smooth bed conditions, further investigations with rough fixed and mobile bed conditions are worthwhile and are reported here.

[1] School of Civil Engineering, The University of Queensland, St Lucia, Brisbane, Queensland, 4072, Australia

The present study focuses on the direct bed shear stress measurements over rough fixed and mobile beds. The basic experiment setup and scenarios will be introduced. Time series of bed shear stress and free surface elevation measurements are compared with previous results and also numerical predictions. Bed shear stress characteristics of different bed configurations are presented and discussed. The directly measured bed shear stress data are then incorporated into the classic Meyer-Peter&Muller (1948) model. The numerical predictions of bed load transport rates are compared with the experimental measurements as well as previous data. Final conclusions are drawn at the end.

EXPERIMENT SETUP

Due to the analogy between dam-break flow and swash flow, dam break experiments have been conducted in the Hydraulic Laboratory at The University of Queensland. The 3-meter flume is made of smooth PVC bed and glass walls. One end of the flume is enclosed, the elevation of which could be adjusted to obtain different beach slopes. An array of five ultrasonic displacement sensors (Mic+25) with a frequency of 50Hz and accuracy of 1mm are deployed in the center of the flume to derive temporal variation of the free surface elevations during the experiments. For the purpose of estimating the pressure gradient contribution, two sensors (Sensor 5 and Sensor 6) have been specially located on top of the two edges of the shear plate. Besides, Sensor 1 has been installed on the dam-break gate to resolve starting time of each run. The basic setup of the dam break experiments is shown in Figure 1.

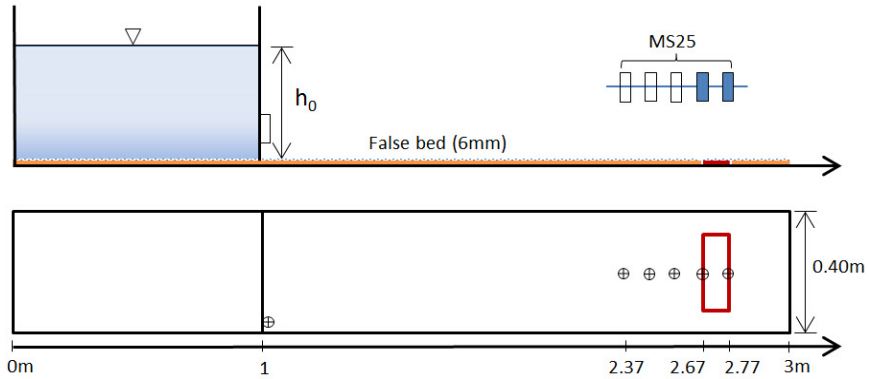

Figure 1. Schematic diagram of dam break experiment setup.

The time series of the swash bed shear stress are directly measured by a flush mounted shear plate (refer to Barnes et al., 2009 for a detailed introduction). The eddy current proximity probe has a sample frequency of 50Hz and resolution of 0.001mm. A pulley/weight system has been designed to obtain the relationship between output voltages and exerted averaged shear stresses (Barnes et al., 2009). The restoring force of the shear plate is provided by the four tubular legs (d=1.1mm) which may be replaced for different research purposes. The calibration has been repeated and finally yields approximately linear curves as in Figure 2. The shear plate has a measurement range of ±82N/m^2. Special attention has been paid to ensure the shear plate is flush with the channel bottom surface and the perimeter of Perspex cell casing.

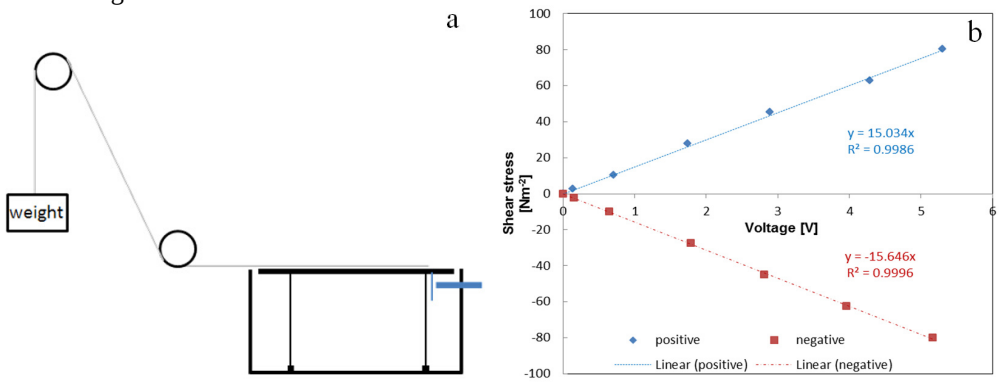

Figure 2. Shear plate calibration. a. Pulley/weight system; b. Calibration curve of averaged shear stress and output voltage signals.

The shear plate used in the present study is 0.1m long, 0.25m wide and 0.75mm thick. Therefore, the bed shear stress obtained in the present study is an area averaged shear stress rather than point measurements. Considering the width of the flume (0.4m), the side wall effects could be ignored.

The dam-break experiments generally include three different types of bed conditions (Figure 3). The smooth bed is made of smooth PVC. And the corresponding bed shear stress measurements have been compared with previous measurements (Barnes, 2009) to make sure that the shear plate works properly. Considering the problem of sediment grains becoming jammed between the shear plate and the box or cumulatively deposited inside the shear box, the sediment sample for rough bed conditions has been sieved and all grains of small size (<2mm) have been excluded. The rough fixed bed therefore consists of a single layer of coarse grains (d_{50}=2.85mm) glued by PVA wood glue while the rough mobile beds include extra mobile grains of different layer thickness. A sediment trap has been placed at the end of the flume to collect sediment overtopping volumes. All experiment scenarios are summarized in Table 1. For each case of the experiment, the measurements have been repeated for at least three times to assess repeatability and variation between runs.

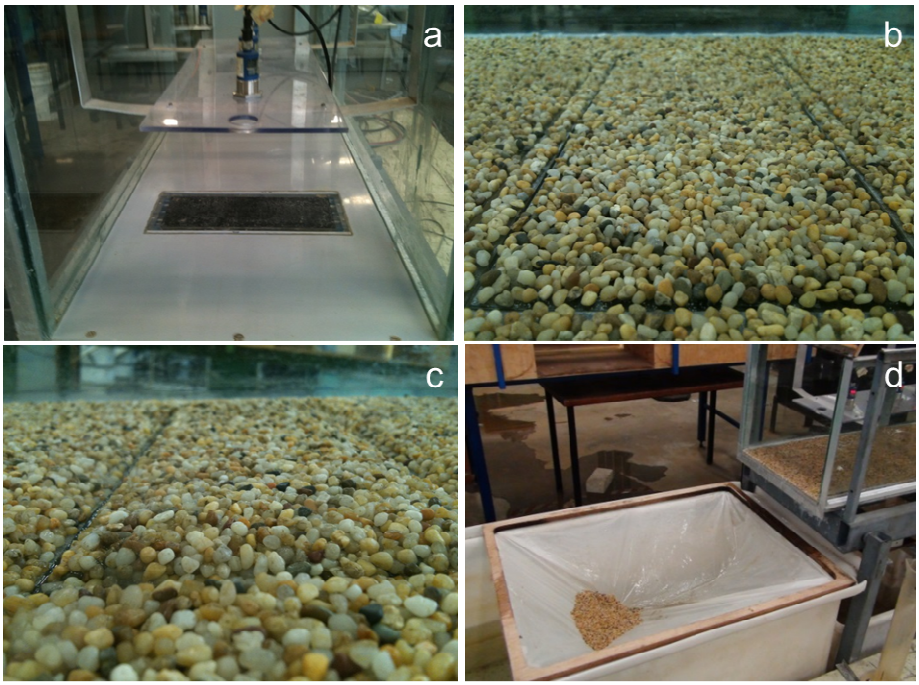

Figure 2. a. Smooth bed; b. Rough fixed bed; c. Rough mobile bed; d. Sediment trap.

Table 1. Summary of shear plate experiment scenarios.

Bed condition	Slope	Reservoir depth [m]	Reservoir length [m]	Grain size [mm]
Smooth	0	0.10, 0.15, 0.20	1.7	-
Rough fixed	0	0.08, 0.10, 0.12, 0.14, 0.16, 0.18, 0.20, 0.22	1.0	2.85
	1:10	0.16, 0.17, 0.18, 0.19, 0.20, 0.21, 0.22		
Rough mobile	0	0.08, 0.10, 0.12, 0.14, 0.16, 0.18, 0.20, 0.22		
	1:10	0.16, 0.17, 0.18, 0.19, 0.20, 0.21, 0.22		

RESULTS

1. Smooth bed results

The dam break experiments with smooth PVC bed have been conducted before applying the shear plate for rough bed conditions. The time series of the free surface elevations and shear stress have been obtained. Due to the difficulties associated with the velocity measurements in the swash flows, a 2D hydrodynamic model (ANUGA, Nielsen et al., 2005) based on finite volume method has been introduced to derive temporal variations of free surface elevations and averaged flow velocities at

specified locations. For both smooth and rough fixed bed conditions, good agreements have been obtained between the free surface elevation measurements and ANUGA predictions, except for some small differences at the early stage of the dam break flow (Figure 4). The main reason is the assumption of hydrostatic pressure distribution (negligible vertical accelerations) used in the numerical model. The influence of the vertical acceleration component could be more significant for locations near the dam gate and mild slope conditions (Freeman and LeMehaute, 1964). Figure 5 shows the comparison of the bed shear stress measurements and previous results of Barnes (2009). Essentially, both the peak shear stress and the starting time have been well reproduced. The bed shears stress decays rapidly after it reaches its peak value.

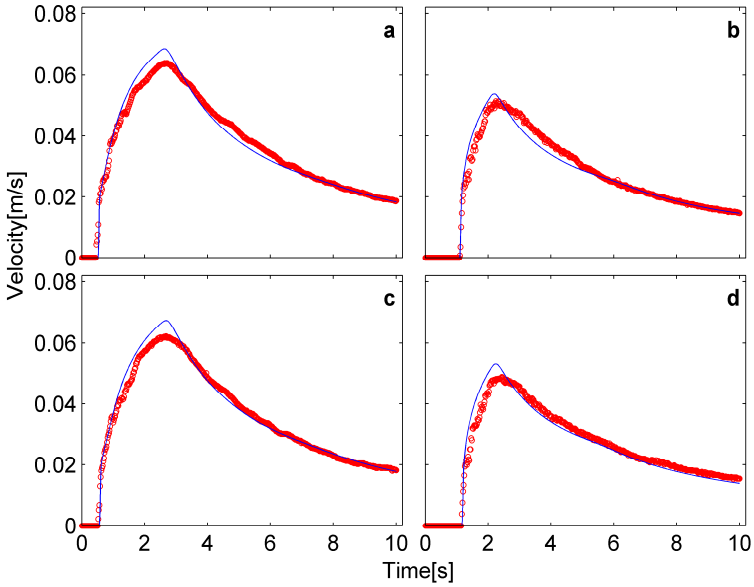

Figure 4. Time series of free surface elevation for sensor 5 (upper) and sensor 6 (lower). Horizontal smooth bed (a and c), L=1.7m, h_0=0.20m; horizontal rough fixed bed (b and d), L=1.0m, h_0=0.20m.

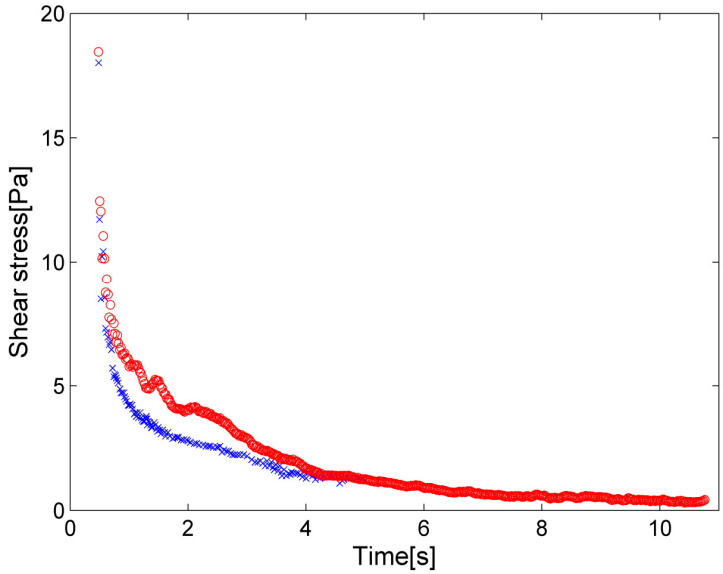

Figure 5. Comparison of bed shear stress between present experiments (red circles) and Barnes (2009, blue crosses). Smooth horizontal bed, L=1.7m, h_0=0.20m.

2. Rough bed results

The total bed shear stress measured in the experiments consists of the skin friction stress and the pressure gradient component, or secondary force (Rankin and Hires, 2000), which acts on the two edges of the shear plate. The contribution of the pressure gradient should be excluded from the measured total shear stress. Previous research indicates that the pressure gradient component shows different characteristics under a wide range of flow regimes. It could be negligible in turbulent boundary layer

flows while on the other hand, be of same order of magnitude with the skin friction shear stress in laminar boundary layer flows (Pujara and Liu, 2014). In the present study, the contribution of the pressure gradient was found to be minor comparing with the skin friction stress.

The pressure gradient component has been subtracted from the measured total bed shear stress as

$$\tau_f = \tau_t - \frac{F_{PG}}{A} = \tau_t + \frac{dp}{dx}\frac{V}{A} \qquad (1)$$

in which V and A are surface area and volume of the shear plate (Barnes et al., 2009), respectively. For horizontal bed cases, dp/dx is negative and the pressure gradient associated force (F_{PG}) acts with the shear stress, while for upward sloping beaches, it always acts in an opposite way (Baldock and Hughes, 2006).

One example has been presented in Figure 6 which demonstrates the temporal variation of the pressure gradient component and the total bed shear stress for mobile bed condition. It is readily noted that the pressure gradient component induced by the seaward dipping water surface (Figure 6a) acts against the shear stress. The magnitude of the pressure gradient component is approximately one order smaller than the measured total bed shear stress (Figure 6b).

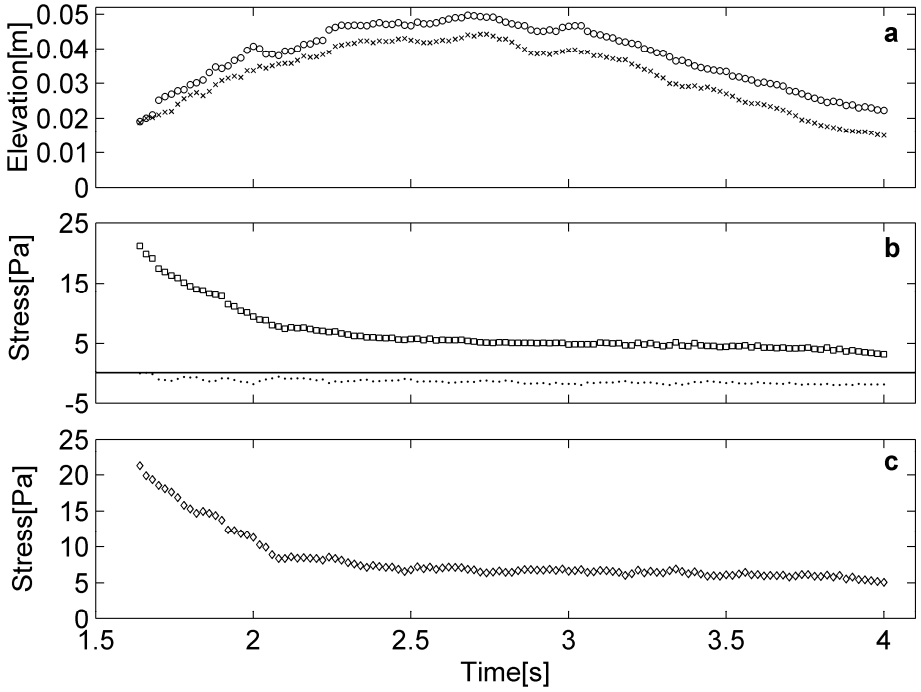

Figure 6. Results of loose mobile bed experiments, L=1.0m, h0=0.20m, S=1:10. a. Variation of the free surface elevation for sensor 5 (crosses) and sensor 6 (circles); b. Variation of measured total bed shear stress (squares) and pressure gradient component (dots); c. Variation of final shear stress.

In order to investigate the influence of varying mobile layer thickness on the bed shear stress, more sediment grains have been added into the flume and carefully distributed evenly over the bed. Figure 7 shows the temporal variation of the bed shear stress according to different layer thicknesses. As the loaded sediment volume increases, the averaged peak bed shear stress increases by about 100%. Meanwhile, the swash front has been slowed down due to the friction force caused by both fixed and mobile sediment grains. For thick layer cases, sediment motions cease and grains settle on shear plate at the late stage of the swash event as the flow slows down. The frictional force generated by these grains eventually impedes the free movement of the shear plate. In some cases, sediment grains will jam in the gap between the shear plate and the box although the sediment samples have been sieved. Either of these two situations will lead to the non-zero residual observed in the dataset. Therefore, the bed shear stress signals have to be truncated and the remaining data would be regarded as unreliable. The duration of trustable shear stress data generally depends on the load volume of mobile sediment grains.

By taking the peak bed shear stress of each repeated run, the averaged peak bed shear stress has been plotted against the initial reservoir water depth in Figure 8 for both horizontal and sloping (1:10) bed conditions. It is noted that the averaged peak bed shear stress increases approximately linearly with

the water depth. For the horizontal bed, the shear plate quickly reaches its measuring capacity when the load volume was increased by 50% at h_0=0.14m. The results of sloping (1:10) bed scenarios show similar patterns but flow velocities are lower. This increase in the bed shear stress can be attributed to the momentum transfer by mobile grains from the swash flow to the bed (Nielsen, 1992) and will be further discussed.

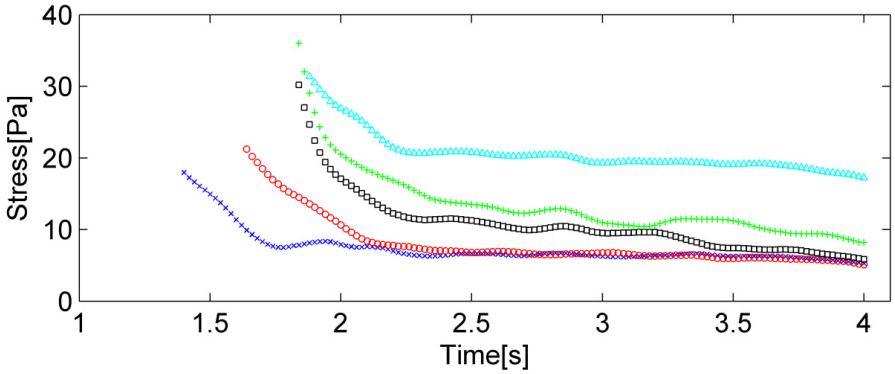

Figure 7. Temporal variation of bed shear stress (S=1:10, h0=0.20m) according to different bed configurations. Crosses, fixed bed; circles, mobile bed; squares, load volume increased by 50%; pluses, load volume increased by 100%; triangles, load volume increased by 150%.

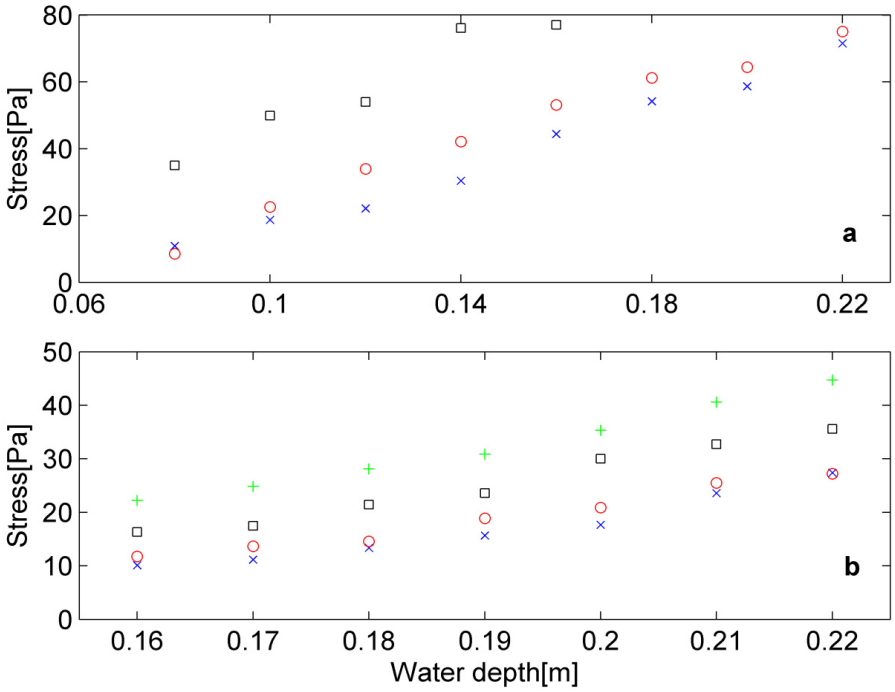

Figure 8. Averaged peak bed shear stress versus initial reservoir water depth for horizontal (upper) and sloping bed (S=1:10, lower) configurations. Crosses, fixed bed; circles, loose mobile bed; squares, load volume increased by 50%; pluses, load volume increased by 100%.

DISCUSSION

As presented above, the averaged peak bed shear stress for mobile bed conditions increases as the load volume increases and the magnitude could be doubled. The measured bed shear stress can be decomposed into two parts: the fluid-related shear stress and the grain borne shear stress (Bagnold, 1956). The significant increase of the bed shear stress under mobile bed configurations is potentially due to the momentum transfer of mobile grains from swash flow to the bed (Nielsen, 1992), i.e. the grain borne shear stress. However, quantitative estimate of this momentum transfer is difficult and quite limited data have been obtained by now.

It is interesting to compare the fluid-driven bed shear stress with that of wind-particles. McKenna and Willetts (1991, 1993) investigated snow saltation and their numerical simulations suggest a considerable increase (as much as 50%) of the shear stress due to snow particle saltation. The wind

tunnel experiments of Nemoto and Nishimura (2000) qualitatively support the numerical simulations and demonstrate that the existence of the saltation layer leads to an increase of the bottom roughness. Full understanding of the role of grain borne shear stress requires accurate velocity measurements of grains in the swash flow, which could be even more challenging in the natural world. On the other hand, numerical models might be an alternative and provide useful insights into this problem.

The measured bed shear stress data has also been directly incorporated into bed load modelling. Due to the fact that very coarse sediment grains (d_{50}=2.85mm) were used in the present experiments, the contribution of the suspended load could be neglected and the classic Meyer-Peter&Muller (1948) bed load formula has been applied in the numerical predictions. The Shields parameter and dimensionless sediment transport flux are calculated as

$$\theta = \frac{\tau}{\rho(s-1)gd} \tag{2}$$

$$\Phi_B = 8(\theta - \theta^{'})^{1.5} \tag{3}$$

in which ρ is the water density; s is the relative density of sediment; τ is the shear stress obtained from the experiments.

Then the total sediment transport rate can be derived as (Nielsen ,1992):

$$Q_B = \Phi_B d\sqrt{(s-1)gd} \tag{4}$$

The sediment transport comparison between the experimental measurements and numerical predictions has been given in Figure 9. Sediment transport data from the same experiment setup but a thicker mobile sediment layer (Othman et al., 2014) have been plotted as well.

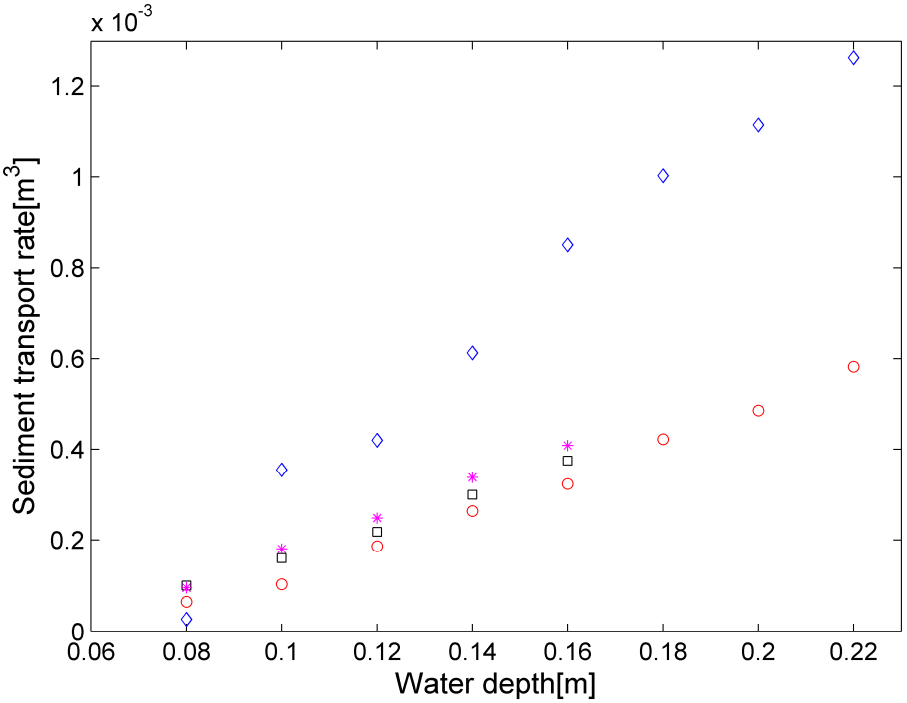

Figure 9. Sediment transport comparison between experimental measurements and numerical predictions of horizontal mobile bed. Circles, mobile bed; squares, load volume increased by 50%; stars, data of Othman et al. (2014); diamonds, numerical predictions based on Meyer-Peter&Muller (1948) formula.

It is readily noted that the total sediment transport rate has been over-estimated by direct incorporation of bed shear stress data. The friction coefficient back-calculated using quadratic drag law and velocity predictions (ANUGA) falls between 0.07 to 0.08, which is higher than the normal values (0.02-0.05) observed in the laboratory and field (Raubenheimer and Elgar, 2004). For constant reservoir water depth, the sediment transport rate increases as more grains have been added into the flume, which indicates starved bed conditions in the present experiments, i.e. limited source of mobile

sediments. This is also justified by the discrepancy between sediment transport data (squares, load volume increased by 50%) and Othman et al. (2014) data which corresponds to unlimited mobile sediments. The deviation between the sediment transport rate and measurements of Othman et al. (2014) is expected to decrease as the load volume increases. The numerical predictions of the sediment transport rate might be improved by combining the shear stress measurements with a Lagrangian hydrodynamic model (Barnes and Baldock, 2010) and will be further investigated in the future work.

CONCLUSIONS

A shear plate has been applied for the direct measurements of bed shear stress over both rough fixed and mobile beds in dam-break driven swash flows. Temporal variations of bed shear stress and free surface elevations have been obtained for different mobile layer thicknesses. Although the reliable time series of bed shear stress could be relatively short as load sediment volume increases, the variation of the bed shear stress during the initial stage of the swash events could be derived. The averaged peak bed shear stress increases approximately linearly with the reservoir water depth. For rough mobile bed conditions, the averaged peak bed shear stress increased to twice that for the rough fixed bed conditions. This might be attributed to the dispersive stress and momentum transfer by added mobile grains from the swash flow to the bed.

The comparison between the sediment transport measurements and previous experiment data (Othman et al., 2014) indicates starved bed conditions in the present research. The direct incorporation of the bed shear stress into the classic Meyer-Peter&Muller (1948) bed load model over-estimates the bed load transportation. Numerical predictions of sediment transport rate might be improved by applying bed shear stress measurements to Lagrangian hydrodynamic models (e.g. Barnes and Baldock, 2010).

REFERENCES

Allis, M., Blenkinsopp, C., et al., 2014. An investigation of log-law theory for estimating swash zone bed shear stress. Coastal Engineering: Subbmitted.

Bagnold, R.A., 1956. The flow of cohensionless grains in fluids. Philosophical Transactions of the Royal Society of London. Series A, Mathematical and Physical Sciences 249(964): 235-297.

Baldock, T.E. and Hughes, M.G., 2006. Field observations of instantaneous water slopes and horizontal pressure gradients in the swash-zone. Continental Shelf Research 26(5): 574-588.

Barnes, M.P., 2009. Measurement and Modelling of Swash Zone Bed Shear Stress. PhD Thesis, The University of Queensland, 184 pp.

Barnes, M.P. and Baldock, T.E., 2010. A lagrangian model for boundary layer growth and bed shear stress in the swash zone. Coastal Engineering 57: 385-396.

Barnes, M.P., O'Donoghue, T., et al., 2009. Direct bed shear stress measurements in bore-driven swash. Coastal Engineering 56: 853-867.

Conley, D.C. and Griffin, J.G., 2004. Direct measurements of bed stress under swash in the field. Journal of Geophysical Research 109(C03050): 1-12.

Cowen, E.A., Sou, I.M., et al., 2003. Particle Image Velocimetry Measurements within a Laboratory-Generated Swash Zone. Journal of Engineering Mechanics 129(10): 1119-1129.

Freeman, J.C. and LeMehaute, B., 1964. Wave breakers on a beach and surges on a dry bed. Journal of Hydraulics Division 90(2): 187-216.

Hanratty, T.J. and Campbell, J.A. (1996). Meaurement of wall shear stress. Fluid Mechanics Measurements. R. J. Goldstein, Taylor&Francs**:** 575-648.

Kolitawong, C., Giacomin, A.J., et al., 2010. Local Shear stress transduction. Review of Scientific Instruments 81(2): 021301.

Li, M.Z., 1994. Direct skin friction measurements and stress partitioning over movable sand ripples. Journal of Geophysical Research 99(C1): 791-799.

McKenna, I.K. and Willetts, B.B., 1993. Adaptation of the near-surface wind to the development of sand transport. Journal of Fluid Mechanics 252: 99-115.

Nemoto, M. and Nishimura, K., 2000. Direct measurement of shear stress during snow saltation. Boundary-Layer Meteorology 100: 147-170.

Nielsen, O., Roberts, S., et al., 2005. Hydrodynamic modelling of coastal inundation. MODSIM 2005 International Congress on Modelling and Simulation, The University of Melbourne, Melbourne, Australia, Modelling and Simulation Society of Australia and New Zealand Inc.

Nielsen, P. (1992). Coastal Bottom Boundary Layers and Sediment Transport. Singapore, World Scientific.

O'Donoghue, T., Pokrajac, D., et al., 2010. Laboratory and numerical study of dambreak-generated swash on impermeable slopes. Coastal Engineering 57(5): 513-530.

Othman, I.K., Baldock, T.E., et al., 2014. Measurement and modelling of the influence of grain size and pressure gradient on swash uprush sediment transport. Coastal Engineering 83: 1-14.

Pope, N.D., Widdows, J., et al., 2006. Estimation of bed shear stress using the turbulent kinetic energy approach—A comparison of annular flume and field data. Continental Shelf Research 26(8): 959-970.

Pujara, N. and Liu, P.L.-F., 2014. Direct measurements of local bed shear stress in the presence of pressure gradients. Exp Fluids 55(1767): 1-13.

Puleo, J.A., Lanckriet, T., et al., 2012. Near bed cross-shore velocity profiles, bed shear stress and friction on the foreshore of a microtidal beach. Coastal Engineering 68: 6-16.

Rankin, K.L. and Hires, R.I., 2000. Laboratory measurement of bottom shear stress on a movable bed. Journal of Geophysical Research 105(C7): 17011-17019.

Raubenheimer, B. and Elgar, S., 2004. Observations of swash zone velocities: A note on friction coefficients. Journal of Geophysical Research 109: C01027.

Riedel, P.H. and Kamphuis, J.W., 1973. A shear plate for use in oscillatory flow. Journal of Hydraulic Research 11(2): 137-156.

Seelam, J.K. and Baldock, T.E., 2010. Measurements and modeling of direct bed shear stress under solitary waves. Proceeding of nineth International Conference on Hydro-Science and Engineering Chennai, India, ICHE 2010.

Sumer, B.M., Sen, M.B., et al., 2011. Flow and sediment transport induced by a plunging solitary wave. Journal of Geophysical Research 116(C01008): 1-15.